34th Annual International Conference of the IEEE EMBS
San Diego, California USA, 28 August - 1 September, 2012

Regional Cardiac Function Assessment In 4D CT: Comparison between SQUEEZ and Ejection Fraction*

Amir Pourmorteza, Karl H. Schuleri, Daniel A. Herzka, Albert C. Lardo, and Elliot R. McVeigh

Abstract— **Recent advances in computed tomography (CT) imaging technology allow fine anatomical structures such as endocardial trabeculae to be resolved. We have developed a method to detect and track such features on the endocardium to extract a measure that reflects local myocardial contraction with minimal human operator interaction. The relative motion of these surface features were used to represent the local contraction of the endocardial surface with a metric we termed "stretch quantifier of endocardial engraved zones" (SQUEEZ). The results were compared against CT function analysis software available through the scanner vendor. SQUEEZ showed significant difference between infarct and remote regions ($p<0.0001$) as verified by delayed enhanced magnetic resonance imaging. The vendor software showed inferior spatial resolution and stair-step artifacts in regional function maps.**

I. Introduction

Few tomographic imaging modalities are capable of producing data with adequate temporal and spatial resolution for detailed regional function assessment. One difficulty with quantitative methods to estimate myocardial function is inability to obtain adequate landmarks in the heart. MR tissue tagging has been validated and is accurate, but it is slow, has poor resolution in the slice selection direction, requires extended breath-holding, and its image analysis is time consuming because of the manual segmentation required to detect the myocardial borders. In addition, the rapidly growing population of patients with implanted pacemakers or implantable cardioverter defibrillators (ICD) are still contraindicated.

Before the advent of volumetric CT, using dynamic spatial reconstructor data, Amini and Duncan proposed a framework for motion tracking of curves and surfaces, based on elastic models and bending energy of a 3D surface, with specific applications to the LV endocardial surface [1].

Recent dramatic advances in CT imaging techniques allow for volumetric imaging of the entire heart with one gantry rotation [2-4].The sub-second acquisition of the entire cardiac volume in 320-row detector CT allows a contrast bolus to be imaged over a short window in the heart cycle with very high spatial resolution fine anatomical structures such as trabeculae on the endocardial surface become visible.

Current methods for CT regional cardiac function analysis involve time consuming manual segmentation, or manual correction of segmentation of the myocardium. These methods generally apply smooth contours to delineate epicardium and endocardium boundaries, thus failing to capture the fine anatomical endocardial structures visible in wide-range detector CT that can be used as landmarks to guide the motion tracking algorithm. Furthermore, these algorithms normally track the 3D motion by analyzing the displacements in stacks of 2D slices and therefore, are prone to through-plane motion artifacts.

We have previously developed an algorithm based on a fast and robust non-rigid registration method [5] to detect and track the fine geometric features on the endocardial surface, which were used to extract a metric that reflects the cardiac muscle contraction. Local changes proportional to the square root of the surface area were computed as a measure of contraction or expansion of the endocardial surface. The method was demonstrated on healthy and chronically infarcted porcine hearts with phase sensitive inversion recovery (PSIR) magnetic resonance (MR) defining the infracted regions of the heart [6]. In this paper we compare the results of our proposed method with a regional cardiac function metric that is currently used in practice.

II. Material and Methods

A. Animal Model

All animal studies were approved by the Johns Hopkins University Institutional Animal Care and Use Committee and comply with the Guide for the Care and Use of Laboratory Animals (National Institutes of Health Publication no. 80-23, revised 1985). Pigs with chronic myocardial infarctions (MI) were created as described in [6]. CT and MRI studies were performed approximately 130 to 180 days after MI induction. A total of 5 infarcted and 3 healthy animals were studied.

B. CT Imaging

Each animal was scanned, with electrocardiographic monitoring, using a 0.5-mm × 320-detector scanner (Aquilion ONE, Toshiba Medical Systems Corporation, Otawara, Japan) at a heart rate < 100 beats/min. During CT acquisition, respiration was suspended and imaging was performed using a retrospectively gated CT protocol with the following parameters: gantry rotation time 350 ms, temporal resolution of up to 58 ms using multisegment reconstruction [4], detector collimation 0.5 mm × 320 (isotropic voxels 0.5× 0.5×0.5 mm^3), tube voltage 120 kV, tube current 400 mA. Images were reconstructed at every 10% of the R-R interval in systole using a standard kernel (FC03), QDS+ noise reduction and a multi-segment (3 to 5-beat) reconstruction algorithm [6].

C. Magnetic Resonance Imaging

In vivo MR images were acquired using a 3T MR scanner (Achieva, Philips, Best, The Netherlands) with a 32-element

A. Pourmorteza (410-955-3131; fax: 410-502-9814; amir.p@jhmi.edu), K.H. Schuleri (kschuleri@jhmi.edu), D.A. Herzka (dherzka1@jhmi.edu), A.C. Lardo (al@jhmi.edu), and E.R. McVeigh (emcveigh@jhu.edu) are with the Johns Hopkins University School of Medicine, Baltimore, MD 21205 USA .

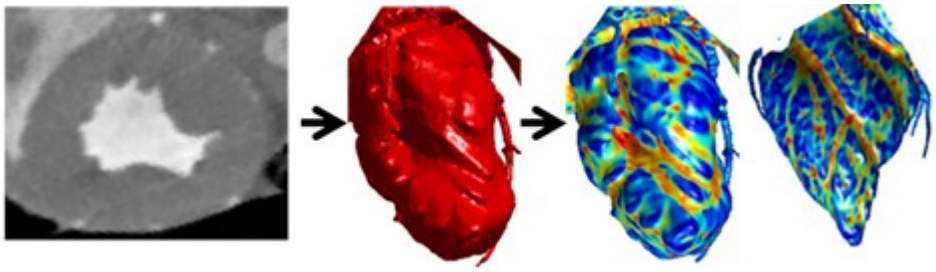

Figure 1: Steps of the proposed method. Left: Short axis CT image of the LV. Note the highly resolved trabecular structures. Middle: Endocardial surface extracted from the CT volumes (inferolateral wall facing viewer). Right: two views of the shape index maps calculated to encode the features engraved by the trabecular structures on the endocardial surface.

cardiac phased array. Myocardial infarct was visualized using late gadolinium enhancement images, acquired 20-25 min after intravenous injection of a double dose of gadolinium diethylenetriaminepenta-acetic acid. A 3D ECG triggered, independent respiratory navigator gated, breath-hold, phase-sensitive inversion recovery gradient echo imaging pulse sequence was used [7]. Imaging field of view (FOV) was 24×24×12 cm^3, with an imaging matrix of 200×195×30, yielding an acquired voxel size of 1.20×1.23×4.0 mm^3, reconstructed to 0.91×.91×2.0 mm^3. Other relevant imaging parameters were: flip angle 15°, TR/TE 5.3/2.6 ms, and 289 Hz/pixel receiver bandwidth.

D. Image Analysis

For each systolic cardiac phase the blood in LV is segmented from the myocardium by thresholding the voxel intensities roughly between 200 HU and 650 HU. After manually pruning the coronaries, and the aorta, a triangulated mesh representing the endocardial surface is extracted from the boundary surface of the LV blood cast (Fig.1).

E. Motion Tracking

We tracked the LV wall motion by calculating trajectories for the points on the endocardial mesh. Each endocardial surface was represented by a triangular mesh. In order to track the points on the meshes from end diastole (ED) to end systole (ES), the surfaces needed to have the same number of triangles with a one to one correspondence between the triangle vertices. This was accomplished by choosing a template mesh (in this case, the ED mesh) and warping it onto a target mesh (any systolic mesh e.g. the ES mesh) such that every triangle on the template mesh has a corresponding triangle on the target mesh [6]. We chose a non-rigid point registration algorithm called coherent point drift (CPD) for surface warping. Coherent point drift is a probabilistic method used for non-rigid surface registration in which surface points are forced to move coherently as a group to preserve the topological structure of the point sets [5].

The registration is considered as a Maximum Likelihood estimation problem, where one point set (template mesh) represents centroids of a Gaussian mixture model (GMM) and the other point set (target mesh) represents the data. CPD algorithm regularizes deformation by penalizing high frequency contents of the deformation field using a Gaussian high-pass filter. In other words, the algorithm penalizes all high order derivatives of the deformation field, whereas thin-plate spline (TPS) algorithms only regularizes first and second-order derivatives of the field. This results in a smoother and more coherent deformation. Compared to similar non-rigid surface registration methods based on TPS deformations [8,9], the CPD regularization can be generalized to nD, whereas for 4D or higher, the TPS kernel solution does not exist. This is especially important when surface features such as curvature metrics or shape measures need to be incorporated as additional dimensions to improve the performance of the algorithm. Furthermore, the locality of spatial smoothness can be controlled by changing the Gaussian filter width, whereas TPS does not have such flexibility.

The choice of Gaussian filters and kernels also allows for reduction of the massive computational burden, associated with high resolution CT datasets, by taking advantage of the fast Gaussian transform. A detailed description of the CPD algorithm and comparison with other point set registration algorithms can be found in [5].

To match the anatomy via surface warping, the homologous anatomical features and their correspondences needed to be identified. Therefore, features engraved on the endocardial surface by fine anatomical structures, such as trabeculae and papillary muscles, were encoded using a scale independent local shape measure, called shape index (SI) (Fig.1), and incorporated in the CPD algorithm to further improve its accuracy. Shape index is a curvature-based measure and for each point is defined by

$$\mathrm{SI} = \frac{2}{\pi} \arctan \frac{k_1 + k_2}{k_1 - k_2} \quad (1)$$

where k1 and k2 are the principal curvatures at that point [10]. The output of the CPD algorithm is a displacement field that is used to calculate measures of local cardiac function. We propose a measure of local cardiac function called Stretch Quantifier of Endocardial Engraved Zones (SQUEEZ), defined as:

$$SQUEEZ(v,t) = \sqrt{\frac{A(v,t)}{A(v,0)}} \quad (2)$$

where A(v,0) is the area of the small triangular patch (v) on the endocardial mesh at end diastole, and A(v,t) is the area of the same patch at time t. SQUEEZ is calculated for each triangular patch on the surface, resulting in a high resolution local cardiac function map of the left ventricle [6].

To compare the results of the proposed method with existing CT cardiac function analysis methods, we analyzed the datasets using Vitrea fX software (Vital Images, Minnetonka, MN), available through Toshiba Medical Systems. Vitrea provides an automatic segmentation which requires manual correction of the endo- and epicardial borders. It produces high resolution bull's-eye plots but only provides quantitative values for 16-segment AHA plots. Vitrea software measures the regional ejection fraction (rEF) defined by

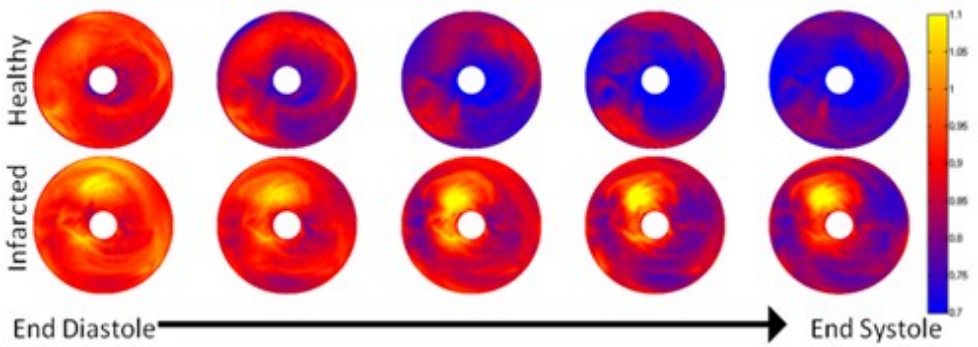

Figure 2: Bull's-eye plots of the SQUEEZ values for one typical healthy (top row), and one infarcted animal (bottom row) from end diastole (left) to end systole (right) at 10% R-R steps. Infarcted animal shows abnormal stretching of the endocardium in LAD territory, anterior and anteroseptal segments, which is consistent with the infarction model (LAD occlusion after the second diagonal) used in this study and confirmed by PSIR MR imaging.

$$\text{rEF\%} = \frac{r_1 - r_2}{r_1} \times 100 \quad (3)$$

where r is the distance of a point on the endocardial contour from a manually selected centerline in a short axis slice at ES (r_2), and ED (r_1).

For a small arc of angle $d\theta$ and length $c = rd\theta$ on the contour, the circumferential shortening can be approximated by

$$\frac{c_1 - c_2}{c_1} = \frac{r_1 d\theta - r_2 d\theta}{r_1 d\theta} = \text{rEF} \quad (4)$$

$$1 - \frac{c_2}{c_1} \cong 1 - \frac{\sqrt{A_2}}{\sqrt{A_1}} = 1 - SQUEEZ \quad (5)$$

In the second line we assumed that, in a small surface element, shortening in an arbitrary direction is almost equal to circumferential shortening. We investigated the following relationship between our SQUEEZ results and the rEF calculated from Vitrea in the 16-segment measurements:

$$SQUEEZ \propto 1 - \text{rEF} \quad (6)$$

Paired two-tailed Student's t-test statistical analysis was performed on the SQUEEZ values to test the difference in the means of the measurements in healthy and infarcted regions. All results are reported in mean±standard deviation.

III. Results

SQUEEZ was calculated for every point on the LV endocardial surface at each cardiac phase (Fig.2). All infarcted animals showed abnormal stretching in the LAD territory, which was consistent with the infarct model used in this work, and was confirmed by the PSIR MR images. Figure 2 shows SQUEEZ bull's-eye plots calculated for 5 consecutive phases from end diastole to end systole. Areas with yellow color (SQUEEZ>1) show abnormal stretch due to myocardial infarction.

Regional ejection fraction was calculated at ES for each cardiac segment using Vitrea. The automatic segmentation of endocardial borders required manual correction which took approximately 150±15 minutes in Vitrea, whereas manual operator interaction needed for SQUEEZ was limited to bulk cropping of the blood-cast in 3D which took 4±2 minutes.

SQUEEZ values are averaged into 16 segments and plotted against the 1-rEF values obtained from Vitrea. The regression plots show good correlation (r=0.81, p<0.001) for the 6 mid-cavity segments, but no correlation was found in basal and apical segments in any of the datasets (Fig. 3).

Vitrea does not provide access to the numerical values of the high resolution bull's-eye plots, therefore we could only compare them to SQUEEZ maps by visual inspection. Although in general the maps look similar, SQUEEZ maps seem to be able to detect wall motion differences at a much higher spatial resolution. This could be attributed to the fact that in Vitrea the number of points on the contours is limited and the contours are smoothed by the segmentation process, therefore they cannot capture the true shape of the endocardial surface. This is especially evident in the dataset shown in Fig.4 where the heterogeneous anterior/anteroseptal infarcted region has sub-regions with different levels of transmurality. SQUEEZ can detect the small heterogeneous sub-regions, whereas the rEF map does not seem to be able to differentiate between different levels of infarct transmurality. Contrast enhanced MR images were used as the gold standard to verify the location of the infracted regions detected in SQUEEZ maps. Points were selected on regions of the endocardial surface near the MI zones as defined by the contrast enhanced MR images. About the same number of points was selected in a remote region of the heart with no sign of MI (Fig.4). The size of the selected regions roughly corresponded to that of one LV segment in the 17-segment AHA model. The average SQUEEZ value was calculated for each zone and showed significant difference (p<0.0001) between MI and non-MI regions in infarcted animals. For healthy animals, a region on the lateral wall was chosen corresponding to the remote non-MI region selected in infarcted animals. The SQUEEZ values for the non-MI in the

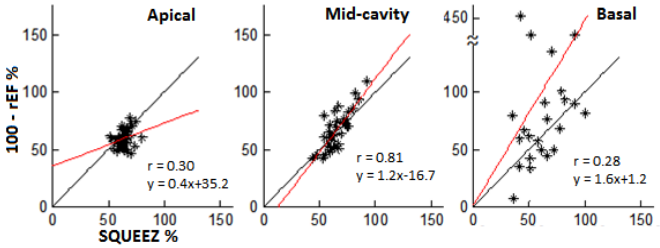

Figure 3: Scatter plots for linear regression analysis between SQUEEZ and rEF measurements for the 16-segment AHA model. From left to right: Basal segments, mid-cavity segments, and apical segments.

infarcted hearts and the regions chosen in the healthy hearts were not significantly different.

IV. Discussion

After Volumetric CT data used in this work can be reconstructed from the routine dose modulated coronary angiography CT scan that is acquired in less than 5 heartbeats. Our method also eliminates the laborious human interaction required to segment the cardiac data for functional

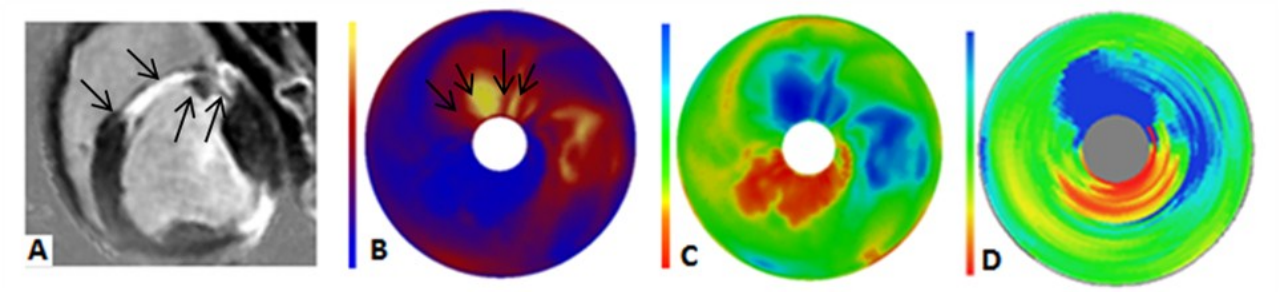

Figure 4**:** A: PSIR image of an animal with an anterior/anteroseptal and an inferolateral infarcted region. The anterior/anteroseptal infarct can be divided into smaller infarcted sub-regions with various levels of transmurality. B and C: End systolic SQUEEZ plots of the same animal, in original SQUEEZ color map (B) and SQUEEZ values in Vitrea color map (C). The short axis slice in (A) corresponds to a concentric circle in the polar plots. The four different levels of transmurality in the small sub-regions are distinguishable in both plots as depicted by the black arrows. D: End systolic regional ejection fraction plot from Vitrea. The small infarcted sub-regions are not visible in this map. Furthermore, the streaks of colors in circumferential direction, especially in anterolateral segments, shown as stair-step artifacts, show the 2D nature of the rEF calculation algorithm.

analysis that has plagued cardiac imaging for the past two decades. Current methods for CT regional cardiac function analysis involve time consuming manual segmentation, or manual correction of segmentation of the myocardium (150±15 min for Vitrea vs. 4±2 min for SQUEEZ). The rEF calculation, by definition, is sensitive to the parameters discussed below.

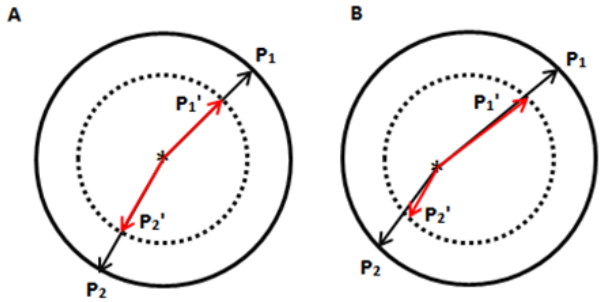

Figure 5: Sensitivity of rEF to center point selection: solid and dashed concentric circles represent endocardial contours at ED and ES, respectively. Assuming uniform radial motion; if the center point is chosen on the center of the circles (A), every point on the contour will have similar rEF values; however, if the center point is misplaced (B) regional function will be underestimated in P_1 and overestimated in P_2.

Initial distance from centerline: Since rEF = $\Delta r/r$, for a constant Δr the regional function is dependent on the initial distance of the point from the centerline. Hence rEF is less sensitive to wall motion in short axis slices in which endocardium has a large radius e.g. basal segments.

Through-plane motion: The longitudinal displacement of tissue into and out of the short axis slice, looks like a change in the endocardial wall position in the short axis slice due to myocardial thickening or stretching, but it in fact is just bulk displacement of tissues in 3D space. The overestimation of regional function in mid-cavity segments (slope=1.2) could be attributed to this artifact (Fig 3). However this artifact is more prominent in basal and apical segments in which the topology of the short axis contours may change significantly due to through-plane motion.

Centerline location: Regional EF calculation is based on distance from a centerline; if the centerline is not chosen correctly, there will be large errors in rEF calculations. This artifact is more prominent in apical slices, where a small change in the position of the centerline could result in very large rEF values (Fig.3-apical). Although the centerlines were chosen carefully, the irregular shape of the contour in apical slices, especially in hearts with chronic infarcts, which have gone under significant LV remodeling, would still cause unrealistically large rEF values in some datasets (Fig.5).

V. Conclusion

Our proposed algorithm, SQUEEZ, outperformed the traditional regional ejection fraction approaches in quantification of regional cardiac function in CT in terms of spatial resolution, operator interaction time, and robustness to through-plane motion artifacts. Although this study showed the proposed method's potential accuracy in detecting small abnormalities, a set of controlled studies of patients with smaller and less transmural infarcts will be forthcoming.

References

[1] A. A. Amini and J. S. Duncan, "Bending and stretching models for LV wall motion analysis from curves and surfaces," *Image and Vision Computing,* vol. 10, pp. 418-430, 1992.

[2] R. George*, et al.*, "Added value of CT myocardial perfusion imaging," *Current Cardiovascular Imaging Reports,* vol. 1, pp. 96-104, 2008.K.

[3] Kitagawa*, et al.*, "Prospective ECG-gated 320 row detector computed tomography: implications for CT angiography and perfusion imaging," *The International Journal of Cardiovascular Imaging,* vol. 25, pp. 201-208, 2009.

[4] K. H. Schuleri*, et al.*, "Applications of cardiac multidetector CT beyond coronary angiography," *Nat Rev Cardiol,* vol. 6, pp. 699-710, 2009.

[5] M. Andriy, "Point Set Registration: Coherent Point Drift," *IEEE Transactions on Pattern Analysis and Machine Intelligence,* vol. 32, pp. 2262-2275, 2010.

[6] A. Pourmorteza, *et al.*, "A New Method for Cardiac Computed Tomography Regional Function Assessment: Stretch Quantifier for Endocardial Engraved Zones (SQUEEZ)," *Circulation: Cardiovascular Imaging,* vol. 5, pp. 243-250, 2012.

[7] P. Kellman*, et al.*, "Phase-sensitive inversion recovery for detecting myocardial infarction using gadolinium-delayed hyperenhancement," *Magnetic Resonance in Medicine,* vol. 47, pp. 372-383, 2002.

[8] N. Lin*, et al.*, "Analysis of Left Ventricular Motion Using a General Robust Point Matching Algorithm" Medical Image Computing and Computer-Assisted Intervention - MICCAI 2003." vol. 2878, R. Ellis and T. Peters, Eds., ed: Springer Berlin / Heidelberg, 2003, pp. 556-563.

[9] F. L. Bookstein, "Principal warps: thin-plate splines and the decomposition of deformations," *Pattern Analysis and Machine Intelligence, IEEE Transactions on,* vol. 11, pp. 567-585, 1989.

[10] J. J. Koenderink and A. J. van Doorn, "Surface shape and curvature scales," *Image and Vision Computing,* vol. 10, pp. 557-564, 1992.